DJS Vol. 51(1) (2025) – pp. 114- 129 ISSN: 1012-5965

Delta Journal of Science

Available online at
https://djs.journals.ekb.eg/

Research Article

CHEMISTRY

Synthesis and photocatalytic activity of zinc oxide/carbon quantum dots and zinc oxide/S-doped carbon quantum dots nanocomposites

Reham S. El-zaablawy[1*], Saleh A. Azim[1], El-Zeiny M. Ebeid[1,2], Samy A. El-Daly[1], Abdelhamid M. El-Sawy[1]

[1] Chemistry Department, Faculty of Science, Tanta University, Tanta, Egypt.
[2] Misr University for Science and Technology (MUST), 6TH of October City, Egypt.

***Corresponding author:** Reham El-zaablawy **e-mail:** reham.shawky@science.tanta.edu.eg

Received: 20/8/2025 **Accepted:** 13/9/2025

KEY WORDS

Carbon quantum dots; heteroatom doping; zinc oxide; photocatalysis; methylene blue degradation.

ABSTRACT

Carbon quantum dots have recently emerged as promising fluorescent nanomaterials due to their wide applications in nanomedicine, bioimaging, biosensing, and photocatalysis. Their unique optical and electrochemical behavior makes them especially attractive for photocatalytic systems. The role of heteroatom-doped CQDs in enhancing the photocatalytic efficiency of ZnO/CQDs nanoparticles is reported. The CQDs, including those doped with heteroatoms, were synthesized via a hydrothermal method, while zinc oxide nanoparticles (ZnO NPs) were produced using a precipitation technique. Composite materials incorporating doped sulfur atoms were fabricated through an impregnation approach at ambient temperature. Structural and morphological characterizations using XRD, FTIR, XPS, TGA, SEM, and TEM confirmed successful fabrication. Photocatalytic experiments revealed that ZnO/S-CQDs achieved a methylene blue (MB) degradation efficiency of up to 79.5%, outperforming other catalysts tested. Furthermore, the band gap energy of pristine ZnO/CQDs (3.01 eV) was reduced to 2.97 eV upon modification with S-CQDs. These findings indicate that although ZnO/CQDs nanocomposite possess a limited photocatalytic response to UV light due to their relatively large band gap, the incorporation of heteroatom-doped CQDs significantly enhances their optical and electronic properties, thereby improving their overall photocatalytic performance.

Introduction

Human health and the environment are at risk due to the increasing presence of organic pollutants in wastewater **(Aboelfetoh et al., 2024)**. Methylene blue (MB) is a major dye used in many industries, including dyeing of wool, silk, paper, textiles, and leather **(El-Ghobashy et al., 2023)**. MB can cause health issues such as eye irritation, breathing problems, confusion, vomiting, and heavy sweating **(Khan et al., 2022)**. In addition, its high solubility in water and resistance to biodegradation make it persistent in aquatic environments, which may lead to long-term ecological damage **(Ali et al., 2014)**. Therefore, it is essential to remove MB from industrial wastewater. Various treatment approaches have been developed, including adsorption, ion exchange, filtration, and photocatalysis. Among them, photocatalytic degradation is particularly advantageous since it completely mineralizes organic pollutants into harmless products like CO_2 and H_2O, while relying on sunlight as the energy source **(Chen and Mao, 2007)**. The process works through the generation of reactive oxygen species such as hydroxyl radicals, photogenerated holes, and superoxide radicals that break down the pollutants efficiently **(Ayu et al., 2023)**. This process is a sustainable and effective method for water purification **(Bahnemann et al., 2004)**.

Recently, ZnO/CQDs have been widely used as photocatalysts due to its low cost, stability, and high reactivity under UV illumination **(Majumder et al., 2020)**. The incorporation of CQDs not only improves photocatalytic efficiency but also helps in extending the light absorption range of ZnO **(Li et al., 2019)**. Furthermore, their photocatalytic activity can be improved by heteroatoms doping, such as sulfur, which introduces electronic states that facilitate charge separation and enhance visible light response **(Teymoorian et al., 2021)**. The quantum characteristics of nanoparticles, determined by their dimensions and electronic configuration, play a vital role in governing the formation of reactive species. Consequently, particle size, surface imperfections, and band gap energy are key parameters that influence their overall activity **(Nawaz et al., 2024)**. In addition, the coupling of CQDs with ZnO generates a heterojunction interface that facilitates electron migration and minimizes charge recombination **(Xiang et al., 2012)**.

CQDs themselves are highly valued for their small size, strong luminescence, biocompatibility, photostability, and ease of surface functionalization **(Ikram et al., 2024)**. This makes them excellent materials for photocatalysis and other nanotechnology applications **(Deb and Chowdhury, 2024)**.

The optical band gap of ZnO/CQDs can be adjusted through variations in particle size, surface properties, or by introducing sulfur atoms. Incorporating heteroatom doping, particularly sulfur, into carbon quantum dots (CQDs) alters the structural and chemical features of ZnO/CQDs, leading to a narrowed band gap that extends absorption into the UV-Vis region, raises the valence band (VB) level, and improves photocatalytic efficiency by promoting electron–hole pair separation **(Li et al., 2013)**. Furthermore, sulfur doping contributes to the creation of additional trap states,

which help extend the lifetime of photoexcited charge carriers.

In this work, ZnO/S-CQDs nanocomposite was prepared by an impregnation method at room temperature. The photocatalytic activity of ZnO/CQDs NPs was significantly enhanced by the introduction of S-CQDs, and their performance was evaluated through the degradation of MB dye as a model pollutant under UV light. The incorporation of sulfur-doped CQDs successfully reduced the band gap energy of ZnO/CQDs from 3.01 eV to 2.98 eV, contributing to improved light absorption and photocatalytic performance.

Experimental Materials

L-ascorbic acid ($C_6H_8O_6$) was obtained from Tianjin Yungda reagent. Sodium thiosulfate pentahydrate ($Na_2S_2O_3.5H_2O$) was supplied by Thermo Scientific chemicals. Methylene blue dye ($C_{16}H_{18}ClN_3S$), methanol (CH_3OH, 99.8%) and isobutanol $(CH_3)_2CHCH_2OH$, 99% were purchased from Sigma Aldrich. Silver nitrate ($AgNO_3$, 99%) was obtained from Alpha Chemika, while Zinc acetate dihydrate $Zn(CH_3COO)_2.2H_2O$ was purchased from Louen reagent. All chemicals were used for analytical grade and applied without further purification.

Synthesis of CQDs and S-CQDs

CQDs were synthesized using L-ascorbic acid as a carbon source. For sulfur doping, sodium thiosulfate pentahydrate was added as a dopant. Specifically, 1.5 mmol of L-ascorbic acid and 0.5 mmol of sodium thiosulfate were dissolved in 20 mL of deionized water under stirring. The solution was then transferred to a Teflon-lined autoclave and heated at 140°C for 4 hours. After cooling, the obtained solution was filtered through a 0.22 μm Mixed Cellulose Ester (MCE) membrane to remove impurities, followed by dialysis (MWCO300 Da) for purification. The same procedure was followed without adding sodium thiosulfate pentahydrate to produce pure L-ascorbic acid–derived CQDs. The resulting CQDs were labeled S-CQDs.

Synthesis of ZnO NPs

ZnO NPs were fabricated through a precipitation route. In brief, 2.195 g of zinc acetate dihydrate was dissolved in 60 mL of deionized water and sonicated for 10 minutes. Separately, 0.8 g NaOH was dissolved in 20 mL of deionized water and added dropwise to the zinc acetate solution with stirring to form a suspension of $Zn(OH)_2$. The precipitate was collected by centrifugation, washed with deionized water, dried at 70°C, and calcined at 140°C for 4 hours to obtain ZnO powder.

Synthesis of CQDs and S-CQDs supported ZnO NPs

The synthesis of CQDs and S-CQDs supported on ZnO NPs was carried out at room temperature using an impregnation technique. Initially, two separate portions of 0.2g ZnO powder were dispersed in 30 mL of anhydrous ethanol and sonicated to form uniform suspensions. Subsequently, 0.5mL and 1mL of dialyzed CQDs solution were individually introduced into each suspension and stirred at 600 rpm for 5 hours in order to investigate the effect of CQDs loading on ZnO NPs. The resulting samples are hereafter denoted as ZnO/CQDs (0.5mL) and ZnO/CQDs (1.0mL). The same procedure was employed to incorporate S-CQDs into ZnO NPs, by adding 0.5 mL and 1.0 mL of the S-CQDs solution to separate suspensions of 0.2 g ZnO NPs and

stirring under identical conditions. These products are referred to as ZnO/S-CQDs (0.5mL) and ZnO/S-CQDs (1.0mL). All obtained nanocomposites were washed, centrifuged, and dried at 80°C overnight.

Photocatalytic decolorization of MB

For the photocatalytic decolorization of MB, 0.05 g of the catalysts were dispersed in 30 mL of a 2.6×10^{-5} M MB solution. The mixture was stirred in the dark for 30 minutes. A 15 W UV lamp placed 20 cm above the solution was used as the irradiation source. During the reaction, 3 mL aliquots were withdrawn every 10 minutes, centrifuged, and analyzed by UV-Vis spectrophotometry at 668 nm. The decolorization efficiency (η%) was calculated according to equation 1:

$$\text{Decolorization (\%)} = [(C_0 - C_t)/C_0] \times 100 \quad \ldots\ldots\ldots\ldots(1)$$

Where C_0 and C_t represent the initial and time-dependent concentrations of MB, based on absorbance values at 668 nm.

Active species trapping experiments

These experiments were designed to identify which species contribute most to the degradation of MB. Isobutanol was used to scavenge hydroxyl radicals ($^{\bullet}OH$), methanol to quench holes (h^+), silver nitrate (0.1 mmol/L) to trap electrons (e^-), and ascorbic acid (0.1 mmol/L) to remove superoxide radicals ($^{\bullet}O_2^-$). The effect of each scavenger on MB degradation efficiency provided insight into the contribution of different reactive oxygen species.

Results and discussion

Instrumental measurements

The synthesized samples, ZnO/CQDs (1 mL) and ZnO/S-CQDs (1 mL) were comprehensively characterized to determine their structural and physical features using multiple analytical techniques. X-ray diffraction patterns were obtained with a GNR APD 2000 PRO diffractometer employing Cu Kα radiation at 40 kV and 30 mA to evaluate crystallinity. Surface topography was explored through scanning electron microscopy (SEM, JEOL JSM-IT200) operated at 10 kV with a magnification of 8000×. High-resolution transmission electron microscopy (HR-TEM, JEOL 2100F, 200 kV) was applied to visualize particle dimensions and lattice fringes. The chemical composition and surface states were analyzed via X-ray photoelectron spectroscopy (XPS, Thermo Scientific K-Alpha, USA). Functional groups were detected using Fourier transform infrared spectroscopy (FTIR, JASCO 4100) with KBr pellets over the 4000–400 cm^{-1} range. Optical absorption properties were examined by UV–Vis spectroscopy (PG T80+ dual-beam spectrophotometer, UK), while fluorescence emission was determined with a JASCO FP-8200 spectrofluorometer. Thermal stability was tested using thermogravimetric analysis (TGA, Perkin Elmer STA6000) between 25 and 900°C at 16°C/min. Finally, photocatalytic efficiency was evaluated under irradiation from a 15 W UV-C lamp (PHILIPS).

Characterization of Catalysts

UV-Vis spectroscopy

UV-Vis spectroscopy was employed to verify the successful formation of CQDs by analyzing their plasmonic resonance behavior, as shown in Fig. (1). The absorption spectra of CQDs synthesized from L-ascorbic acid, along with those doped with heteroatoms such as sulfur, displayed bands in the range of 220–330 nm. Two main absorption peaks were present in the CQD spectra. The

peak at 220 nm is due to the n→π* transition of C=O groups, while the shoulder peak at 275 nm corresponds to the π→π* transition of C=C in aromatic rings. Small shifts and increase in intensity confirm the successful synthesis of CQDs and their modification by doping different heteroatoms **(Liu et al., 2024)**.

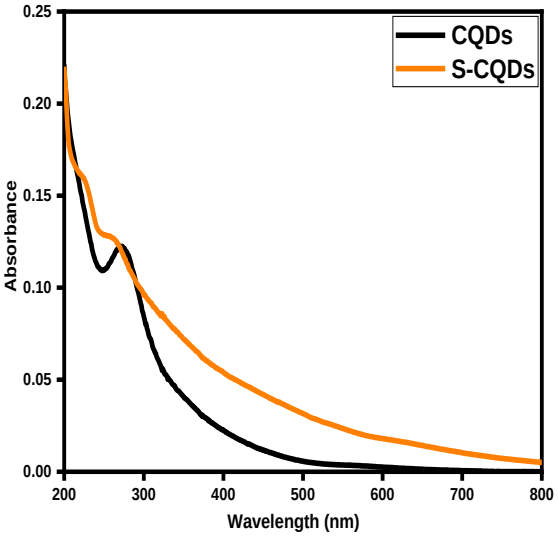

Fig. (1): UV-Vis absorption spectra of CQDs and S-CQDs aqueous solutions.

Fluorescence spectra

Fluorescence spectrum provides insight into the emission behavior of CQDs and S-CQDs, as shown in Fig. (2), with all samples measured under the same conditions. Quantum yield (QY), a key indicator of fluorescence efficiency, was calculated relative to quinine sulfate (QY = 0.54 in 0.1 M H_2SO_4, excited at 240 nm using equation **(Ayu et al., 2023)**. Among the samples, S-CQDs exhibited the highest QY (0.157), due to enhanced surface passivation and radiative transitions. This was followed by CQDs (QY = 0.057), demonstrating the significant role of sulfur doping in improving fluorescence properties.

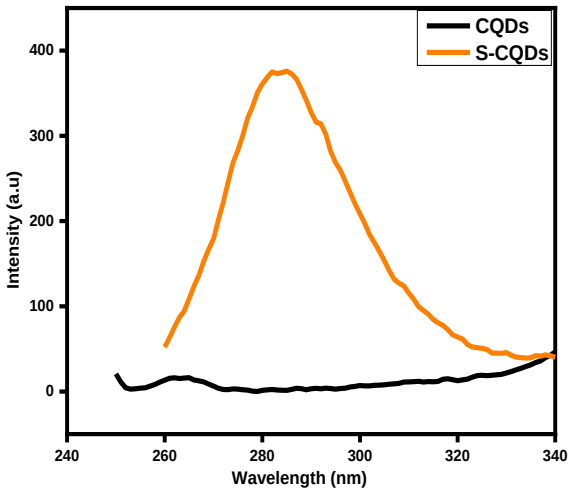

Fig. (2): Fluorescence spectra of CQDs and S-CQDs (λ_{ex} = 240 nm).

FTIR analysis

FTIR confirmed the bonding features of the composites. In Fig. (3), for ZnO/CQDs, characteristic peaks appeared at 460 cm^{-1}, related to stretching vibrations of Zn–O bonds. In CQDs, peaks at 3410 cm^{-1} and 2930 cm^{-1} were assigned to O–H and C–H stretching vibrations, while peaks at 1087 cm^{-1}, 1400 cm^{-1}, and 1640 cm^{-1} indicated C–O, C=C and C=O functional groups, respectively **(Liu et al. 2022)**. For S-CQDs, the peaks at 890 cm^{-1} refer to the C=S functional group. These FTIR results confirm the successful doping of sulfur atom into the CQD structures, and their attachment to the ZnO surface **(Liu et al., 2024)**.

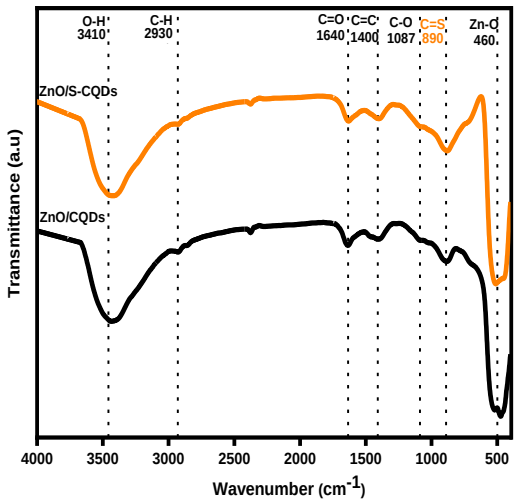

Fig. (3): FTIR spectra for ZnO/CQDs and ZnO/S-CQDs NPs.

XRD analysis

XRD patterns were used for comparing the crystalline structures of various zinc oxide (ZnO)-based quantum dot composites. The composites include ZnO with carbon quantum dots (ZnO/CQDs), and CQDs doped with sulfur (ZnO/S-CQDs). Two samples show characteristic peaks corresponding to the hexagonal wurtzite structure of ZnO/CQDs, with planes indexed as (100), (002), (101), (102), (110), (103), (200), (112), and (201), in Fig. (4a). These peaks indicate that the crystal structure of ZnO/CQDs is preserved after the incorporation of S dopant, though slight shifts and intensity variations in some peaks suggest lattice distortion or changes in crystallinity due to doping as shown in Fig. (4b) **(Montero-Muñoz et al., 2020)**.

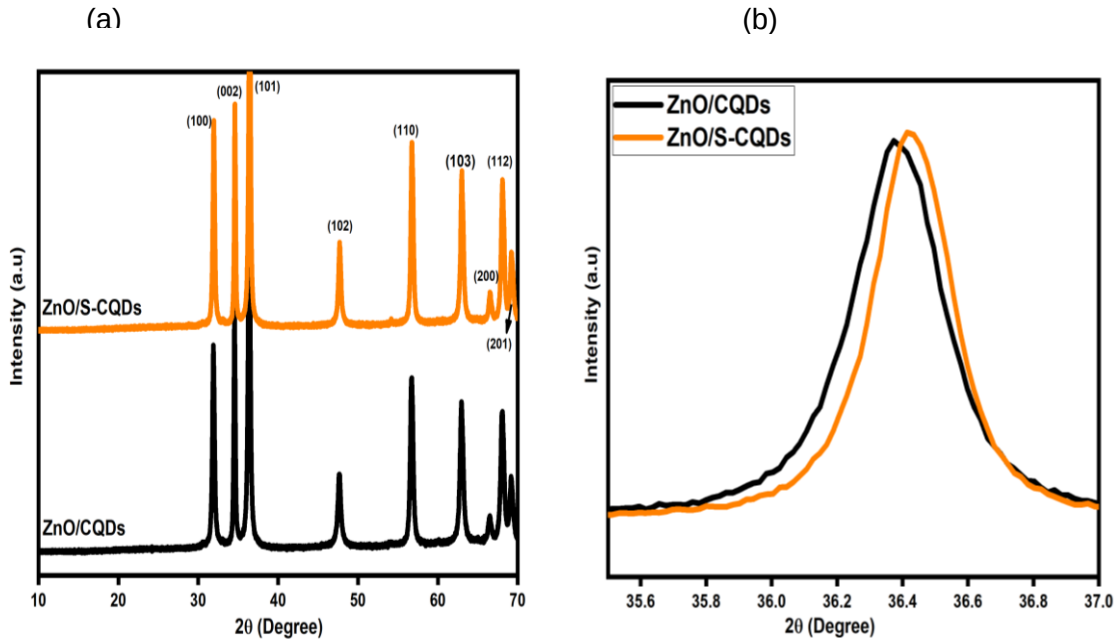

Fig. (4): (a) XRD of ZnO/CQDs and ZnO/S-CQDs NPs, (b) XRD patterns of the samples peak (101)

XPS analysis

To determine the surface chemistry and elemental makeup of the obtained nanocomposites (ZnO/CQDs and ZnO/S-CQDs), XPS characterization was carried out. In Figure 5(a), the survey spectrum confirms the presence of elements Zinc (Zn 2p), oxygen (O 1s) and carbon (C 1s). In Figure 5(b), Zn 2p spectrum exhibited four distinct signals in the ranges of 1022.85-1025.41 and 1045.76-1048.62 eV, related to Zn $2p_{3/2}$ and Zn $2p_{1/2}$, which are consistent with Zn^{+2} ions in the tetrahedral Zn-O lattice **(Kadam et al., 2021)**. In Fig. 5(c), O 1s spectrum displayed two peaks at

532.1eV and 534.17eV, assigned to oxygen bonded within Zn-O as well as adsorbed oxygen or hydroxyl groups. Additionally, the C 1s spectrum revealed three peaks at 284.74 eV, 286.92 eV and 290.32 eV, representing C-C/C=C, C-O and O=C-O bonds, verifying the existence of various oxygen-containing carbon groups in Fig. 5(d). The overall XPS results strongly support the incorporation of CQDs into the ZnO matrix along with associated chemical state modifications **(Bozetine et al., 2016)**. Fig. 6(a) shows the survey spectra of Zn 2p, O 1s, C 1s and S 2p3 from ZnO/S-CQDs. In Fig. 6(b), C 1s spectrum shows peaks at 284.74 eV, 286.85 eV and 289.09 eV, corresponding to C-C/C=C, O=C-O, and C=S/C-O bonds, respectively, which confirm the functionalization of S-CQDs. In Fig. 6(c), S 2p3 spectrum shows two peaks at 164.05 eV ascribed to S 2p of thiophene-S and 168.19 eV indicated that some sulfur exists in the form of C-SOx species in the ZnO/S-CQDs. These results collectively indicate that sulfur doping in CQDs have been effectively incorporated into the ZnO matrix **(Liu et al., 2024)**.

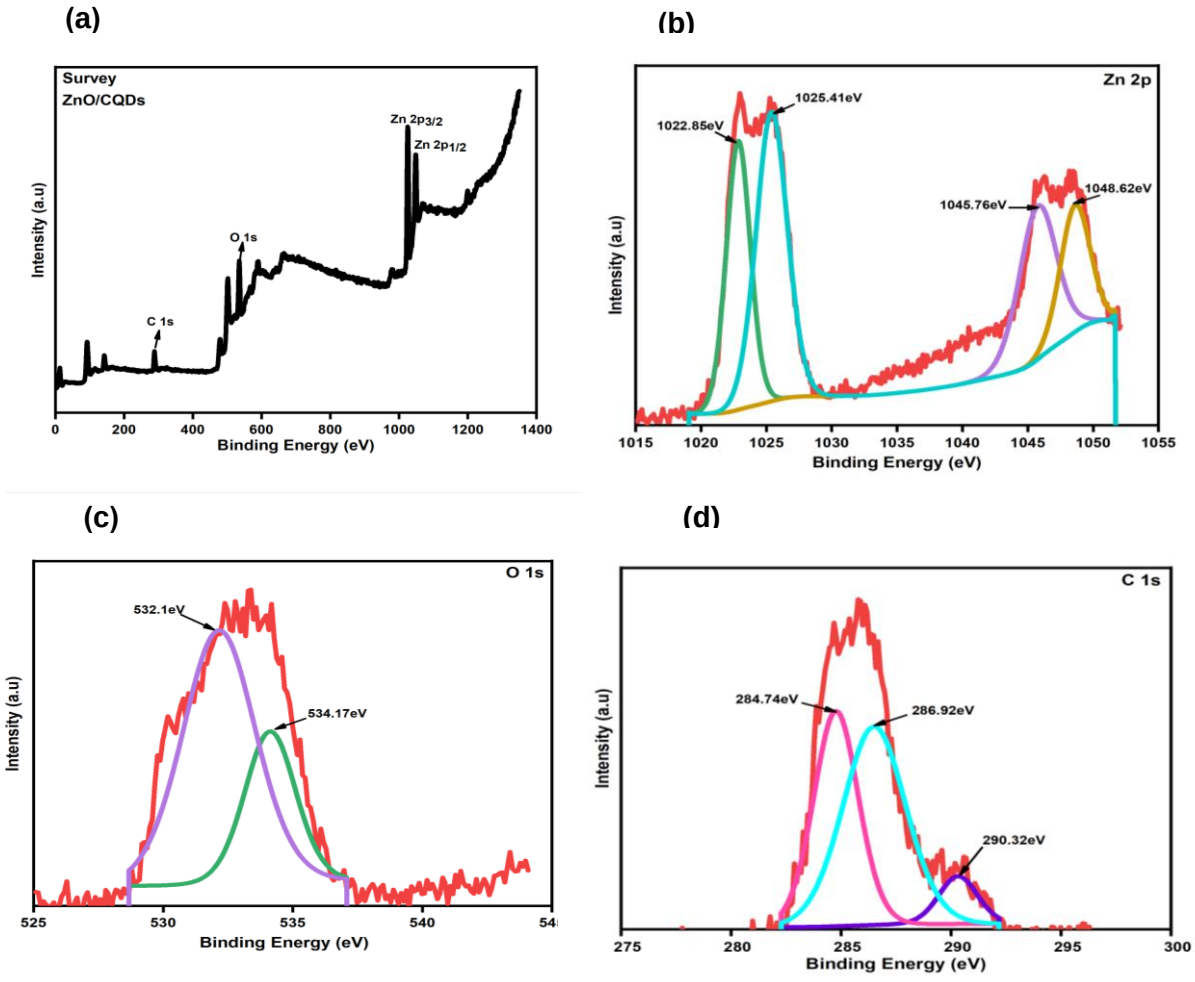

Fig. (5): (a) XPS full survey of ZnO/CQDs and high-resolution spectra of (b) Zn 2p, (c) O 1s, (d) C 1s.

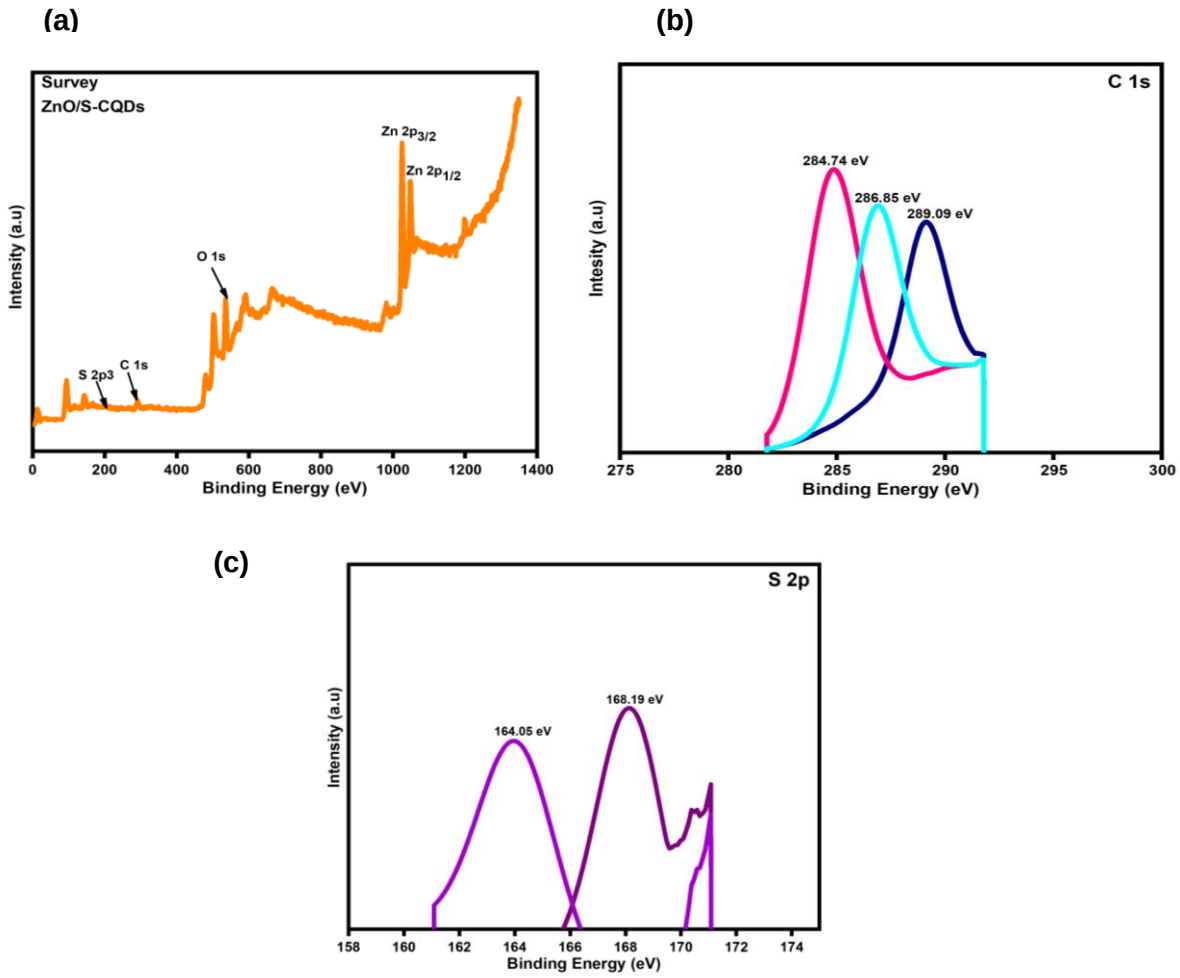

Fig. (6): (a) XP S full survey of ZnO/S-CQDs and high-resolution spectra of (b) C 1s, (c) S 2p3.

TGA analysis

TGA curves show the thermal stability of ZnO/CQDs and ZnO/S-CQDs **(del Campo et al., 2021)**. In Fig. (7), ZnO/CQDs exhibit a significant weight loss starting from around 200°C due to the degradation of organic groups and surface species attached to CQDs. This is reflected by a weight drop of 4.7 % by 300°C and a further 1.17% by 400°C, after which the weight stabilizes at about 92%. In contrast, ZnO/S-CQDs show much greater stability, with only a small weight loss of 0.6% up to 500°C, retaining nearly their initial mass afterwards. This improved stability is due to sulfur-doping, which strengthens the structure and reduces the number of removable surface groups and defects.

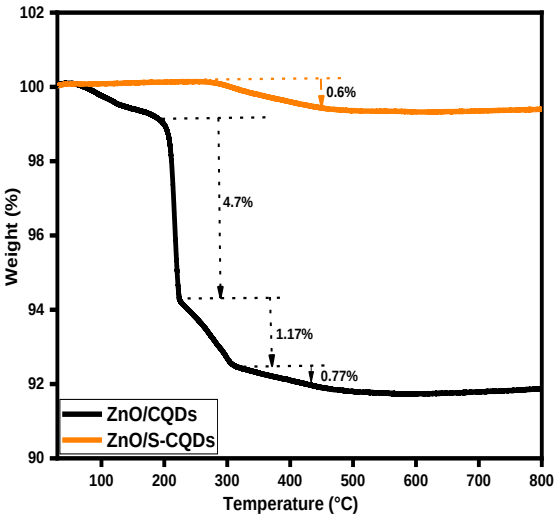

Fig. (7): TGA thermograms of ZnO/CQDs and ZnO/S-CQDs.

UV-Vis absorption spectra and band gap energies

Figure (8) demonstrates the UV-Vis absorption characteristics of ZnO/CQDs and ZnO/S-CQDs solutions. The absorption edge (where absorbance sharply drops) shifts with dopant. This shift is key for determination of the band gap energy (E_g) using Tauc plot method in Fig. (9). ZnO/CQDs show the highest band gap of 3.01 eV, which is typical for ZnO/CQDs due to its wide energy separation between the valence and conduction bands **(Liu et al., 2024)**. When combined with sulfur in doped S-CQDs, the band gap slightly decreases to 2.97 eV as S-CQDs. This slight narrowing of the band gap can be ascribed to the incorporation of sulfur atoms, which introduces additional electronic states near the conduction or valence bands. This, in turn, narrows the energy gap and allows for absorption of lower-energy photons, thereby improving the photocatalytic activity under ultraviolet light irradiation.

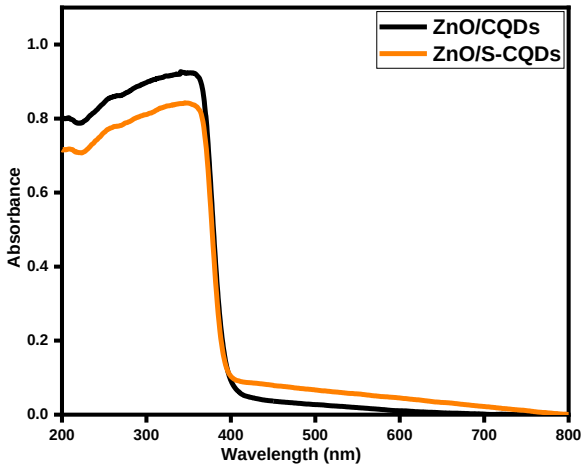

Fig. (8): UV-Vis absorption spectra of aqueous ZnO/CQDs and ZnO/S-CQDs solutions.

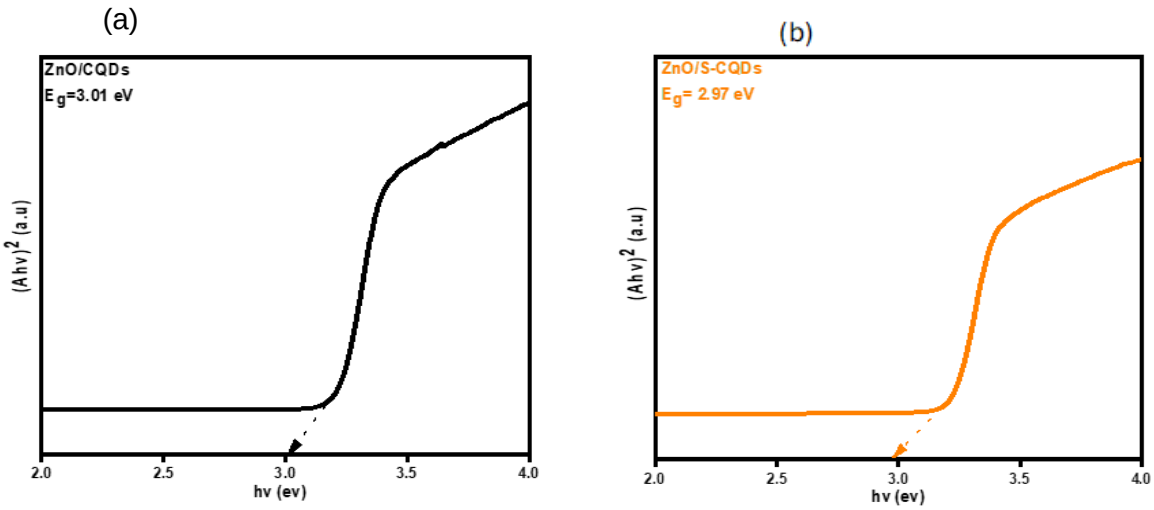

Fig. (9): Band gap energy (a) ZnO/CQDs and (b) ZnO/S-CQDs

SEM analysis

The surface morphology of ZnO/CQDs and ZnO/S-CQDs were investigated using SEM. In image 10(a), the ZnO/CQDs sample displays a relatively dense and aggregated structure with fewer visible pores, indicating limited surface roughness and a moderate dispersion of CQDs on the ZnO matrix. The Sulfur doped composite (ZnO/S-CQDs, image 10(b) exhibits a more porous and loosely packed morphology, with a rougher surface texture and finer particle distribution. This notable

difference can be attributed to S doping, which enhances the interaction between the CQDs and ZnO, promoting better dispersion, and increasing surface area. These morphological features of ZnO/S-CQDs are favorable for photocatalytic applications, as they facilitate improved light harvesting, greater pollutant adsorption, and more efficient generation of reactive species factors that collectively contribute to its enhanced photocatalytic performance, as supported by previous studies **(Rahman and Kar, 2020)**.

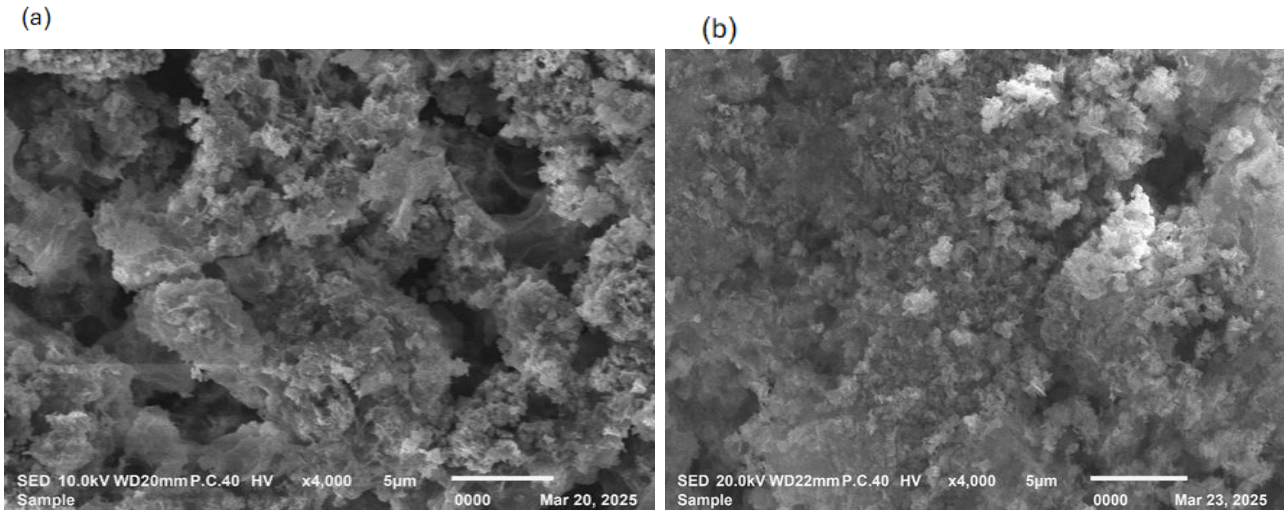

Fig. (10): SEM images of (a) ZnO/CQDs and (b) ZnO/S-CQDs.

TEM analysis

Figure (11) shows images of the synthesized nanocomposites: ZnO/CQDs (a) and ZnO/S-CQDs (b). ZnO/CQDs image shows relatively aggregated and irregularly shaped ZnO NPs, with sizes around 50–200 nm. The CQDs appear to be uniformly attached to the ZnO surface, likely enhancing surface area and electron transport. In contrast, image 11(b) depicts ZnO/S-CQDs, where sulfur-doped CQDs are incorporated. This image reveals more dispersed and finer particle distribution, with distinct size annotations ranging from ~15 nm to ~110 nm, indicating better dispersion and possible improvement in surface interaction due to sulfur doping. The smaller and more uniform particles suggest enhanced quantum confinement and photocatalytic potential. The differences indicate that sulfur doping in CQDs significantly modifies the morphology and interaction with ZnO, which could lead to improved optical or electronic properties **(Wang et al., 2014)**.

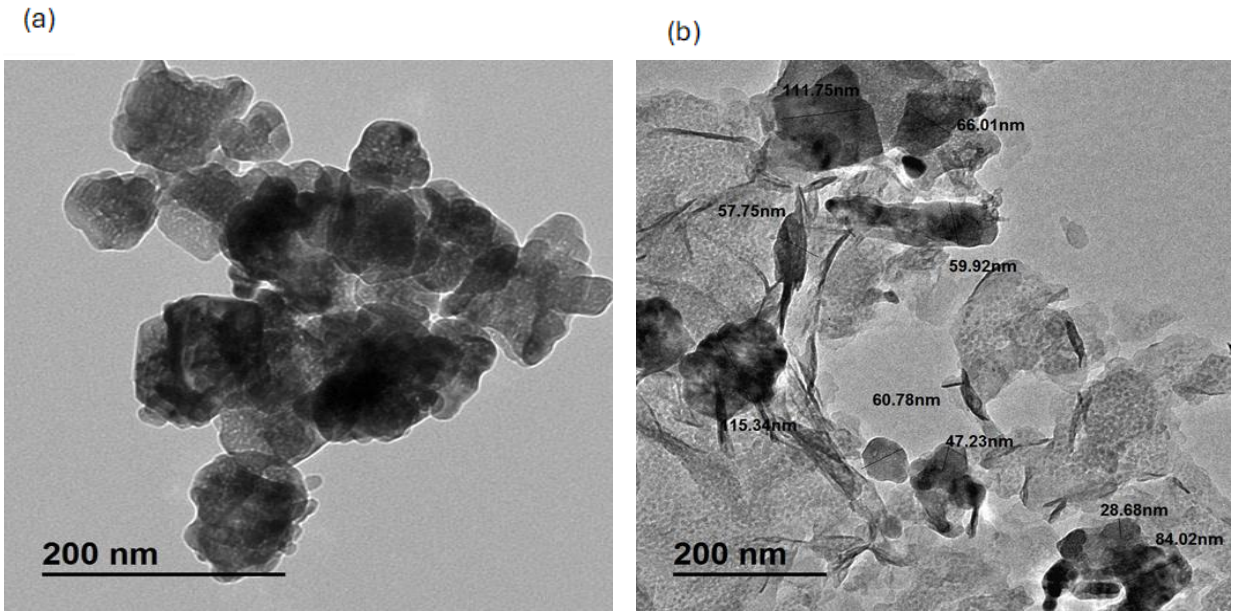

Fig. (11): TEM images of (a) ZnO/CQDs and (b) ZnO/S-CQDs.

Photocatalytic performance analysis

Study on photocatalytic performance

The photodecolorization experiments were performed to identify the most effective catalyst for MB removal. The performance of ZnO/CQDs (0.5 mL, 1mL), and ZnO/S-CQDs (0.5 mL, 1 mL) were evaluated under identical operating conditions. The reaction system was prepared with $[MB]_o$= 6.58 mg/L, catalyst dose= 0.05 g, neutral pH= 7 at 30°C and stirring in the dark for 30 minutes. After that, photocatalytic activity was initiated using a 15 W Ultra-violet lamp. The light source was positioned approximately 20 cm away from the reaction surface. The photocatalytic efficiency of ZnO-based nanocomposites was investigated through the degradation of MB under UV irradiation. As shown in Fig. (12a), ZnO/S-CQDs (1mL) composite demonstrated the highest photocatalytic performance, followed by ZnO/CQDs (1 mL), ZnO/S-CQDs (0.5 mL), and finally ZnO/CQDs (0.5 mL), which showed the lowest activity. All catalysts exhibited an initial adsorption phase in the dark, followed by a sharp decline in MB concentration once the light source was switched on. The kinetic data followed a Pseudo-first-order, with the rate constants (k) calculated and presented in Fig. (12b) as 0.002 min^{-1}, 0.006 min^{-1}, 0.05 min^{-1}. And 0.012 min^{-1} for ZnO/CQDs (0.5mL), ZnO/CQDs (1mL), ZnO/S-CQDs (0.5mL), and ZnO/S-CQDs (1mL), respectively. These results confirm that both sulfur doping and increasing S-CQDs content significantly enhance the photocatalytic degradation efficiency by improving charge separation, increasing light absorption, and providing more active sites for the reaction.

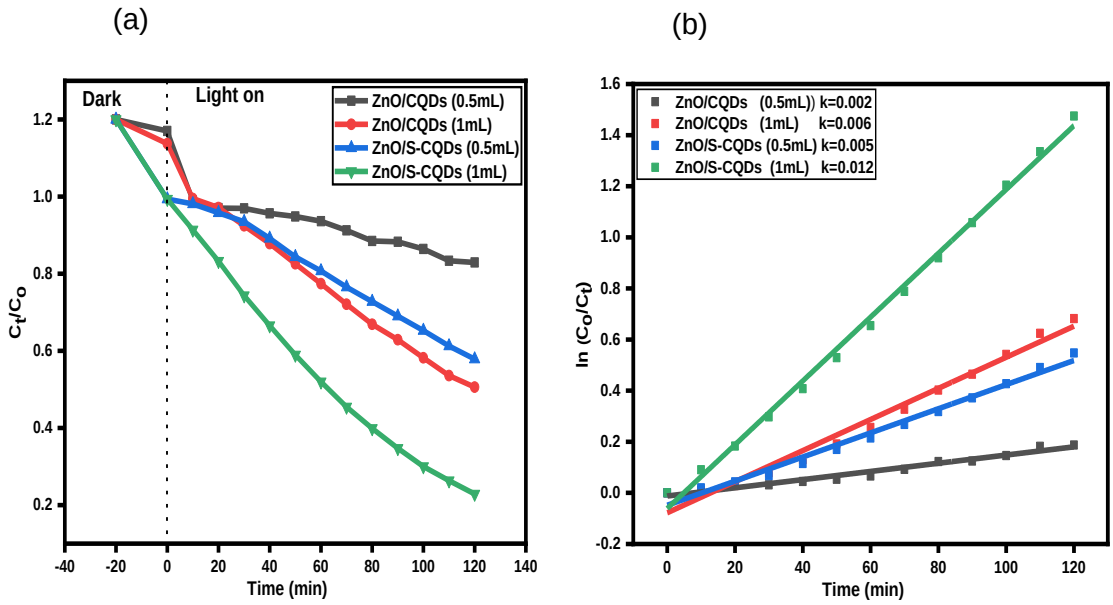

Fig. (12): (a) Decolorization of ZnO/CQDs and ZnO/S-CQDs. (b) Pseudo-first-order kinetic represents the degradation curve.

Effect of doses

As shown in Fig. (13a), increasing the catalyst amount from 0.03 g to 0.04 g resulted in a marked rise in MB removal efficiency, from 53.4% to 79.5%. This enhancement can be explained by the greater availability of active surface sites, improved adsorption of dye molecules, and the formation of additional reactive radicals during the process. In contrast, when the dose was further raised from 0.05 g to 0.06 g, the degradation efficiency dropped slightly from 77.1 % to 75.4 %. This decline is likely due to the excessive amount of catalysts, which may block light penetration and reduce the activation of the photocatalyst, thus limiting the formation of reactive species. Therefore, the optimal catalyst dose for maximum decolorization was identified as 0.04 g **(Liu et al., 2024)**.

Analysis of active free radicals formed during photocatalysis

Under UV illumination, the photocatalytic decolorization of MB by ZnO/S-CQDs proceeds through the production of multiple reactive oxygen species (ROS). As demonstrated by the scavenging experiments in Fig. (14), superoxide radicals ($^{\bullet}O_2^-$) and hydroxyl radicals ($^{\bullet}OH$) play the most crucial roles in the degradation process. The introduction of L-ascorbic acid, a selective scavenger for superoxide radicals ($^{\bullet}O_2^-$), resulted in the most substantial decrease in degradation efficiency (from 79.5% to 48.7%), highlighting $^{\bullet}O_2^-$ as the primary reactive species. Similarly, the use of isobutanol, a scavenger for $^{\bullet}OH$, reduced the degradation efficiency to 51.2%, confirming the secondary, yet significantly active, $^{\bullet}OH$ radicals. In contrast, the addition of silver nitrate (an electron scavenger) and methanol (a hole scavenger) caused only minor decreases in activity, suggesting that the direct roles of electrons (e^-) and holes (h^+) are less critical compared to the ROS-mediated pathway.

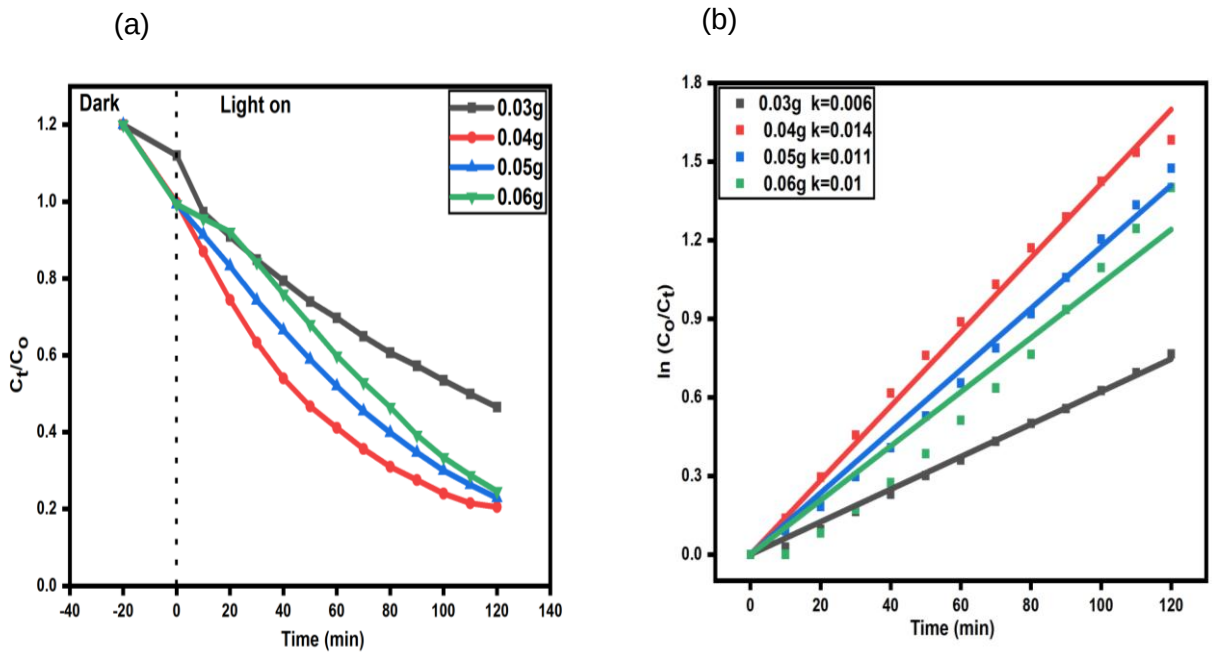

Fig. (13): (a) Decolorization of MB using different doses of ZnO/S-CQDs. (b) Pseudo-first-order kinetic represents the degradation curve.

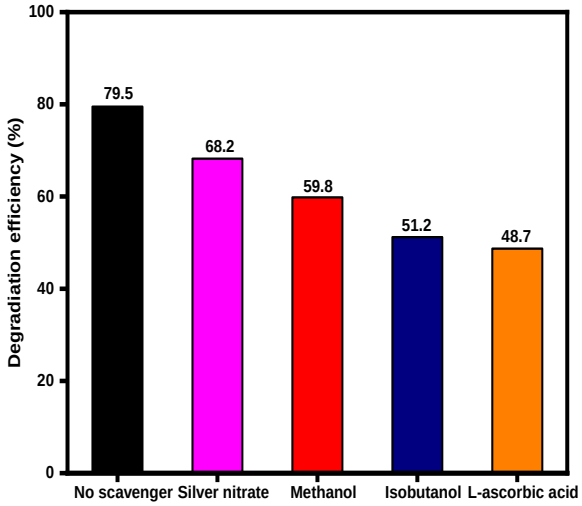

Fig. (14): The free radicals scavenging during the photocatalytic decolorization of MB.

Analysis of photocatalytic reaction mechanism

The optical characterization and photocatalytic activity of ZnO/S-CQDs system demonstrate that incorporation of S-CQDs narrows the band gap energy compared to ZnO/CQDs, enhances light-harvesting ability, promotes better photon utilization, and facilitates more efficient electron transfer. These factors collectively lower the overall energy barrier for the photocatalytic reaction. The proposed mechanism begins with the dark phase, where S-CQDs bond to ZnO surface act as active adsorption sites, concentrating MB molecules near the catalyst surface. Upon exposure to UV light, both ZnO and S-CQDs become photoexcited, thereby generating electron–hole pairs according to equation (2). The photogenerated electrons from ZnO are rapidly transferred to S-CQDs, which helps prevent electron–hole recombination. These transferred electrons then interact with dissolved oxygen molecules on the S-CQDs surface to form superoxide radicals ($^{\bullet}O_2^-$) according to equation (3). Simultaneously, holes in the valence band of ZnO transfer to the surface and oxidize water molecules or hydroxide ions, producing hydroxyl radicals ($^{\bullet}OH$) as equation (4). These reactive oxygen species, particularly $^{\bullet}O_2^-$ and $^{\bullet}OH$, are

primarily responsible for breaking down and mineralizing MB into harmless small molecules as in equation (5).
The overall reactions are shown as follows.

$$ZnO + h\nu \rightarrow h^+ + e^- \quad (2)$$
$$e^- + O_2 \rightarrow {}^{\bullet}O_2^- \quad (3)$$
$$h^+ + H_2O/OH^- \rightarrow H^+ + {}^{\bullet}OH \quad (4)$$
$$Dye + {}^{\bullet}O_2^- / {}^{\bullet}OH \rightarrow CO_2 + H_2O \quad (5)$$

Reusability of ZnO/S-CQDs

To evaluate the reusability of the ZnO/S-CQD (1mL) nanocomposite, it was recovered by filtration after MB decolorization. The nanocomposite was then immersed in 100 mL of an ethanol-water solution (1:1) and continuously stirred at 140 rpm for 12 hours. Afterwards, it was filtered again, thoroughly washed, and dried at 60°C before reused in subsequent photocatalytic tests. This regeneration process was repeated for four cycles to determine the stability and reusability of the nanocomposite. The photocatalytic stability of the ZnO/S-CQDs (1mL) nanocomposite was tested over four cycles of MB decolorization at 6.58 mg/L. The decolorization efficiency decreased from 79.5% in the first cycle to 52.8% by the fourth cycle Fig. (15), indicating a partial loss of activity. The retained performance may be attributed to the self-cleaning capability of S-CQDs, which helps preserve surface activity. The observed decline is likely due to surface fouling by dye residues or leaching of CQDs/S-CQDs during recovery, highlighting areas for future improvement in catalyst stability.

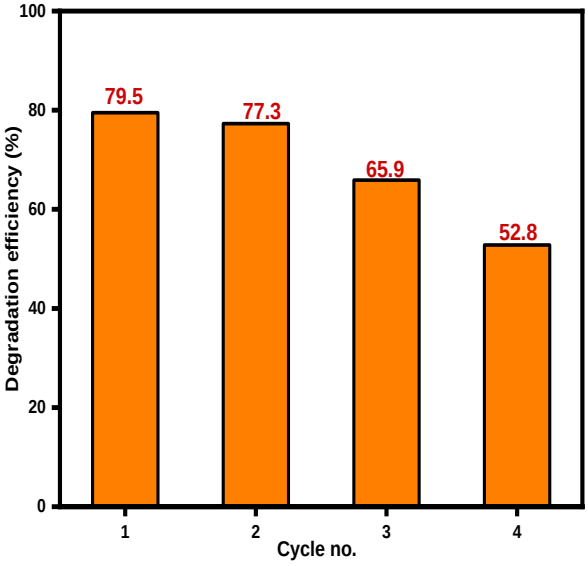

Fig. (15): Reusability of the ZnO/S-CQDs (1mL) for MB decolorization. Dose = 0.04 g, $[MB]_o$ = 6.58 mg/L, pH= 7, Temperature = 30 °C.

Conclusion

In summary, two novel nanocomposites ZnO/CQDs and ZnO/S-CQDs, were successfully synthesized through a simple room-temperature impregnation method. ZnO/S-CQDs demonstrated superior photocatalytic performance in degrading MB under UV light. This enhanced activity is attributed to the synergistic effects of surface functionalization, improved electron transfer, and photon up-converted provided by the S-CQDs. With their low cost, simple synthesis process, high degradation efficiency, and notable stability, these nanocomposites hold great promise for wastewater treatment.

Reference

Aboelfetoh, E. F., Rabea, M. F., El-Sheikh, M. Y., and Okba, E. A. (2024). In situ polymerization of acrylamide on magnetic $SnFe_2O_4/CeO_2$ nanocomposite: A novel adsorbent for removing various dyes. *J. Mol. Struct.*, 1312, 138566.

El-Ghobashy, M. A., Salem, I. A., El-Dahrawy, W. M., and Salem, M. A.

(2023). Fabrication of α-MnO_2/Fe-Mn binary oxide nanocomposite as an efficient adsorbent for the removal of methylene blue from wastewater. *J. Mol. Struct.*, 1272, 134118.

Khan, I., Saeed, K., Zekker, I., Zhang, B., Hendi, A. H., Ahmad, A., Ahmad, S., Zada, N., Ahmad, H., and Shah, L. A. (2022). Review on methylene blue: Its properties, uses, toxicity and photodegradation. WA., 14(2), 242.

Ali, I. (2014). Water treatment by adsorption columns: evaluation at ground level. *Sep. Purif. Rev*., 43(3), 175-205.

Chen, X., and Mao, S. S. (2007). Titanium dioxide nanomaterials: synthesis, properties, modifications, and applications. *Chem. Rev*., 107(7), 2891-2959.

Ayu, D. G., Gea, S., Andriayani, Telaumbanua, D. J., Piliang, A. F. R., Harahap, M., Yen, Z., Goei, R., and Tok, A. I. Y. (2023). Photocatalytic degradation of methylene blue using N-doped ZnO/carbon dot (N-ZnO/CD) nanocomposites derived from organic soybean. *ACS omega*, 8(17), 14965-14984.

Bahnemann, D. (2004). Photocatalytic water treatment: solar energy applications. *Sol. Energy*., 77(5), 445-459.

Majumder, S., Chatterjee, S., Basnet, P., and Mukherjee, J. (2020). ZnO based nanomaterials for photocatalytic degradation of aqueous pharmaceutical waste solutions–A contemporary review.*Environ. Nanotechnol. Mon. Ma nage*., 14, 100386.

Li, J., Liu, K., Xue, J., Xue, G., Sheng, X., Wang, H., Huo, P., and Yan, Y. (2019). CQDS preluded carbon-incorporated 3D burger-like hybrid ZnO enhanced visible-light-driven photocatalytic activity and mechanism implication. *J. Catal*., 369, 450-461.

Teymoorian, T., Hashemi, N., Mousazadeh, M. H., and Entezarian, Z. (2021). N, S doped carbon quantum dots inside mesoporous silica for effective adsorption of methylene blue dye. *SN Appl. Sci.*, 3(3), 305.

Nawaz, A., Farhan, A., Maqbool, F., Ahmad, H., Qayyum, W., Ghazy, E., Rahdar, A., Diez-Pascual, A. M., and Fathi-karkan, S. (2024). Zinc oxide nanoparticles: Pathways to micropollutant adsorption, dye removal, and antibacterial actions-A study of mechanisms, challenges, and future prospects. *J. Mol. Struct*., 1312, 138545.

Xiang, Q., Yu, J., and Jaroniec, M. (2012). Graphene-based semiconductor photocatalysts. *Chem. Soc. Rev*., 41(2), 782-796.

Ikram, Z., Azmat, E., and Perviaz, M. (2024). Degradation efficiency of organic dyes on CQDs as photocatalysts: A review. ACS omega, 9(9), 10017-10029.

Deb, A., and Chowdhury, D. (2024). Biogenic carbon quantum dots: Synthesis and applications. *Curr. Med. Chem.*, 31(25), 3899-3924.

Li, Y., Zhang, B.-P., Zhao, J.-X., Ge, Z.-H., Zhao, X.-K., and Zou, L. (2013). ZnO/carbon quantum dots heterostructure with enhanced photocatalytic properties. *Appl. Surf. Sci.*, 279, 367-373.

Liu, H., Du, K., and Sun, H. (2024). Optimization, Kinetics, and Thermodynamics Study on the Degradation of RhB by ZnO Modified with Nitrogen and Sulfur Co-Doped Carbon Quantum Dots. *Water Air Soil Pollut.*, 235(2), 111.

Liu, H., Li, H., Du, K., and Xu, H. (2022). Photocatalytic activity study of ZnO modified with nitrogen–sulfur co-doped carbon quantum dots under visible light. *New J. Chem.*, 46(31), 14867-14878.

Montero-Muñoz, M., Ramos-Ibarra, J. E., Rodríguez-Páez, J., Marques, G., Teodoro, M., and Coaquira, J. (2020). Growth and formation mechanism of shape-selective preparation of ZnO structures: correlation of structural, vibrational and optical properties. Phys. Chem. Chem. Phys., 22(14), 7329-7339.

Kadam, S. A., Thomas, S. A., Ma, Y.-R., Jose, L. M., Sajan, D., and Aravind, A. (2021). Investigation of adsorption and photocatalytic behavior of manganese doped zinc oxide nanostructures. Inorg. *Chem. Commun.*, 134, 108981.

Bozetine, H., Wang, Q., Barras, A., Li, M., Hadjersi, T., Szunerits, S., and Boukherroub, R. (2016). Green chemistry approach for the synthesis of ZnO–carbon dots nanocomposites with good photocatalytic properties under visible light. *J. Colloid Interface Sci*., 465, 286-294.

del Campo, A., De Lucas-Gil, E., Rubio-Marcos, F., Arrieta, M. P., Fernández-García, M., Fernandez, J. F., and Muñoz-Bonilla, A. (2021). Accelerated disintegration of compostable Ecovio polymer by using ZnO particles as filler. Polym. Degrad. Stabil., 185, 109501.

Rahman, K. H., and Kar, A. K. (2020). Effect of band gap variation and sensitization process of polyaniline (PANI)-TiO_2 pn heterojunction photocatalysts on the enhancement of photocatalytic degradation of toxic methylene blue with UV irradiation. *J. Environ. Chem. Eng.*, 8(5), 104181.

Wang, Y., and Hu, A. (2014). Carbon quantum dots: synthesis, properties and applications. *J. Mater. Chem. C*, 2(34), 6921-6939.

التحضير ونشاط التحفيز الضوئي لمركبات نانوية من أكسيد الزنك/النقاط الكربونية الكمية وأكسيد الزنك/النقاط الكربونية الكمية المطعمة بالكبريت.

ريهام الزعبلاوي[١]، د. صالح عبد العظيم[١]، د. الزيني عبيد [١،٢]، د. سامي الدالي [١]، د. عبد الحميد الصاوي [١]

[١]قسم الكيمياء، كلية العلوم، جامعة طنطا، طنطا، مصر
[2] جامعة مصر للعلوم والتكنولوجيا، مدينة ٦ أكتوبر، مصر.

ظهرت النقاط الكربونية الكمية مؤخرًا كمواد نانوية فلورية واعدة نظرًا لتطبيقاتها الواسعة في الطب النانو، والتصوير الحيوي، والاستشعار الحيوي، والتحفيز الضوئي. وتُعد خصائصها البصرية والكهروكيميائية الفريدة جذابة بشكل خاص في أنظمة التحفيز الضوئي. تم في هذا العمل الإبلاغ عن دور النقاط الكربونية الكمية المطعمة بالذرات غير المتجانسة في تعزيز الكفاءة الضوئية التحفيزية لجسيمات أكسيد الزنك/النقاط الكربونية الكمية النانوية. تحضير النقاط الكربونية الكمية، بما في ذلك المطعمة بذرات غير متجانسة، باستخدام الطريقة الحرارية المائية، بينما تم تحضير جسيمات أكسيد الزنك النانوية بطريقة الترسيب. كما جرى تصنيع المواد المركبة المطعمة بذرات الكبريت بتقنية التشريب عند درجة حرارة الغرفة. أكدت تقنيات التوصيف البنيوي والمورفولوجية (مطيافيه الاشعة تحت الحمراء بتحويل فورييه، حيود الأشعة السينية، مطيافية الالكترونات بالأشعة السينية، التحليل الوزني الحراري، المجهر الالكتروني الماسح، المجهر الالكتروني النافذ) نجاح عملية التحضير.

كشفت التجارب التحفيزية الضوئية أن أكسيد الزنك/النقاط الكربونية الكمية المطعمة بالكبريت حقق كفاءة في تحلل الميثيلين الأزرق بلغت تسعة وسبعون ونصف بالمائة، متفوقًا على بقية المواد المحفزة. علاوة على ذلك، انخفضت فجوة الطاقة أكسيد الزنك/النقاط الكربونية الكمية النقي من 3.01 الكترون فولت إلى ٢,٩٧ الكترون فولت بعد التعديل باستخدام النقاط الكربونية الكمية المطعمة بالكبريت. تشير هذه النتائج إلى أنه رغم أن أكسيد الزنك/النقاط الكربونية الكمية النانوية يمتلك استجابة محدودة للضوء فوق البنفسجي بسبب فجوة الطاقة الكبيرة نسبيًا، فإن دمج النقاط الكربونية الكمية المطعمة بالذرات غير المتجانسة يعزز بشكل ملحوظ خصائصها البصرية والإلكترونية، مما يحسن من أدائها التحفيزي الضوئي العام.